Measurements of scattering and absorption changes in muscle and brain

ENRICO GRATTON[1], SERGIO FANTINI[1], MARIA ANGELA FRANCESCHINI[1], GABRIELE GRATTON[2] AND MONICA FABIANI[2]

[1] *Laboratory for Fluorescence Dynamics, University of Illinois at Urbana-Champaign, 1110 W. Green St., Urbana, IL 61801, USA*
[2] *Department of Psychology, University of Missouri, 210 McAlester Hall, Columbia, MO 65211, USA*

SUMMARY

Non-invasive techniques for the study of human brain function based on changes of the haemoglobin content or on changes of haemoglobin saturation have recently been proposed. Among the new methods, near-infrared transmission and reflection measurements may have significant advantages and complement well-established methods such as functional magnetic resonance imaging and positron emission tomography. Near-infrared measurements can be very fast, comparable in speed to electrophysiological measurements, but are better localized. We will present the demonstration of measurements of millisecond signals due to brain activity in humans following stimulation of the visual cortex. However, major unresolved questions remain about the origin of the signals observed. Optical measurements on exposed cortex in animals show that both the absorption and the scattering coefficient are affected by neural activity. Model calculations show that the signals we detected may originate from rapid changes of the scattering coefficient in a region about 1 to 2 cm below the scalp. We discuss our measurement protocol, which is based on a frequency-domain instrument, and the algorithm to separate the absorption from the scattering contribution in the overall optical response. Our method produces excellent separation between scattering and absorption in relatively homogeneous masses such as large muscles. The extrapolation of our measurement protocol to a complex structure such as the human head is critically evaluated.

1. INTRODUCTION

One of the major advances in the understanding of light propagation in tissues was the demonstration that the diffusion approximation of the Boltzmann transport equation was reasonably well satisfied under a range of typical physiological conditions (Ishimaru & Patterson 1978; Fishkin *et al*. 1991; Patterson *et al*. 1989). Together with this theoretical and experimental result, during the past ten years there has been tremendous progress in optical techniques, including the availability of short-pulsed lasers in the near-infrared. It was soon realized that the information content of a time-resolved measurement in a uniform scattering medium (Patterson *et al*. 1989) was sufficient to separate the contribution of scattering and absorption to the light attenuation in tissues. At the same time, it was proposed that the frequency-domain technique, which intrinsically contains the same information as the time-resolved measurement, may result in faster acquisition times and cheaper instrumentation (Fishkin *et al*. 1991). One of the major differences between frequency and time domain is that in the frequency domain the measurement at a single modulation frequency can be sufficient to isolate the contribution of the scattering from that of the absorption. This is strictly true for homogeneous media, and for measurement locations far from the light source. However, in several practical situations the measurement of the front of the photon density wave must be performed relatively close to the source, or the source terms may be poorly determined. A few years ago we proposed to use a variant of the single-frequency method, the multidistance method, which avoids some of the problems related to the source term, but has some other restrictions in practical applications. In this article we discuss (i) the hardware used in the frequency-domain instrument, (ii) the implementation of the multidistance method for the measurement of absorption and scattering in homogeneous media and (iii) the application of fast acquisition techniques for the measurement of transient signals associated with neuronal activity.

2. PHOTON DENSITY WAVES

When working in the frequency domain, it is useful to think of light propagating in a turbid medium in terms of photon density waves. These waves of light intensity modulated at high frequency travel at constant velocity in the medium. Photon density waves display some of the optical phenomena associated with waves such as reflection, refraction and diffraction (O'Leary *et al*. 1992). The velocity of the propagation

of the photon density waves and their attenuation in the turbid medium depend on the medium optical parameters. In particular, the photon density $U(t)$ of the wave at a detector point at the distance r from the source has the following expression valid in the diffusion regime in an infinite and homogeneous medium (Fishkin & Gratton 1993):

$$U(t) = \frac{S}{4\pi v D r}\left(\mathrm{e}^{-r\sqrt{(\mu_a/D)}} + A\mathrm{e}^{-kr}\mathrm{e}^{\mathrm{i}(\Phi_0-\omega t)}\right) \equiv U_{DC} + U_{AC}, \mathrm{e}^{\mathrm{i}(\Phi_0-\omega t)}, \quad (1)$$

where ω is the angular modulation frequency, r is the source–detector separation, v is the speed of light in the medium, D is the diffusion coefficient which is defined as $1/(3\,\mu_s')$ where μ_s' is the reduced scattering coefficient, μ_a is the absorption coefficient, $k = \sqrt{[(v\mu_a - \mathrm{i}\omega)/(vD)]}$, Φ_0 is the phase of the source A, its modulation depth and S its strength. From equation (1), the value of the phase Φ and the amplitude U_{AC} of the wave can be calculated taking the argument (for the phase) and the absolute value (for the amplitude) of U_{AC}. The average value of the photon density is given by U_{DC}.

$$\Phi = r\sqrt{\left(\frac{\mu_a}{2D}\right)}\left[\sqrt{(1+x^2)} - 1\right]^{\frac{1}{2}}, \quad (2)$$

$$\ln(rU_{DC}) = r\left[-\sqrt{\left(\frac{\mu_a}{D}\right)}\right] + \ln\left(\frac{S}{4\pi v D}\right), \text{ and} \quad (3)$$

$$\ln(rU_{AC}) = r\left[-\sqrt{\left(\frac{\mu_a}{2D}\right)}\right]\left[\sqrt{(1+x^2)} + 1\right]^{\frac{1}{2}} + \ln\left(\frac{SA}{4\pi v D}\right), \quad (4)$$

$$\text{where} \quad x = \frac{\omega}{v\mu_a}, \quad (5)$$

$$\text{and} \quad D = \frac{1}{3\mu_s}. \quad (6)$$

What is important is that from the value of the phase Φ and amplitude U_{AC} (or U_{DC}) of the wave it is possible to extract the values of the reduced scattering and absorption coefficient of the medium. In the next section we discuss how to measure accurately the values of the phase and attenuation of the photon density wave.

3. FREQUENCY-DOMAIN INSTRUMENTATION

The basic design of our frequency-domain instrument follows the lines of the multifrequency-phase fluorometer developed in our laboratory about 15 years ago (Gratton & Limkeman 1983; Gratton *et al.* 1984). Since the light modulation frequency is of the order of 100 MHz, it is still difficult to measure the phase and the modulation of the light at this high frequency with high precision. In fact, to measure accurately changes in haemoglobin saturation of the order of 2–3 %, we estimate that we need to measure the phase and the amplitude of the photon density wave with an accuracy of about 0.5° of phase and 0.4 % of the amplitude of the wave. Using current technology, this accuracy can be easily achieved if the light intensity is adequate. To better appreciate this point, let us consider what is the source of noise in the measurement of the photon density wave. It has been shown (Pogue 1995) that the only source of noise in the commercial frequency-domain instrument by ISS Inc. is due to photon statistics. This instrument is built on the design of our instrument described in 1987. Based on the so-called four-phase measurement illustrated in figure 1, the uncertainty of the phase and amplitude measurement can be computed from the number of counts (photon detected) in each of the four-phase bins and assuming photon statistics. Consequently, to reach an accuracy of the phase of about 0.5°, we need a total of about 4000 counts in the four bins (French 1996).

Of course, this estimate varies depending on the effective modulation of the signal and figure 1 is based on 100 % source modulation. The accuracy in the determination of the absorption and scattering coefficients depends also on systematic measurements errors. Systematic errors are much more difficult to account for. We have followed a 'calibration procedure' by which we determine the response of our system for a calibration sample for which we know (from independent measurements) the optical properties. Then the measurement in the tissue represents only a relatively small perturbation with respect to the pre-calibrated value. Using the calibration protocol, most of the systematic errors are avoided or strongly reduced (Fantini *et al.* 1995).

4. THE MULTIDISTANCE METHOD

One of the major problems encountered in the practical application of the measurement of the absorption and scattering parameters of turbid media using the front of the photon density wave is that the so-called 'source terms', i.e. the phase and the amplitude of the source are not exactly known. In addition, even if the phase and the amplitude of the source are exactly known, the description of the light transport in the multiple scattering medium is well described by the diffusion approximation only far from the source. We have shown that the extrapolation of the photon density wave phase measured far from the source back to the source can give values of the phase that are unphysical, i.e. negative values. This apparent contradiction is due to the approximation used to describe the propagation of the photon density wave. However, after travelling for a distance of about 7–8 mm from the source, the propagation of the photon density wave is well described by the diffusion approximation (Fantini *et al.* 1997). Since at those larger distances, the photon density wave travels at constant velocity and attenuates like an exponential divided by the distance, the phase as a function of distance and the logarithm of the amplitude (DC or AC) multiplied by the distance, are described by three straight lines (see equations (2)–(4)). The phase, DC and AC straight lines are associated with the corresponding slopes S_Φ, S_{DC} and S_{AC}. From each one of a

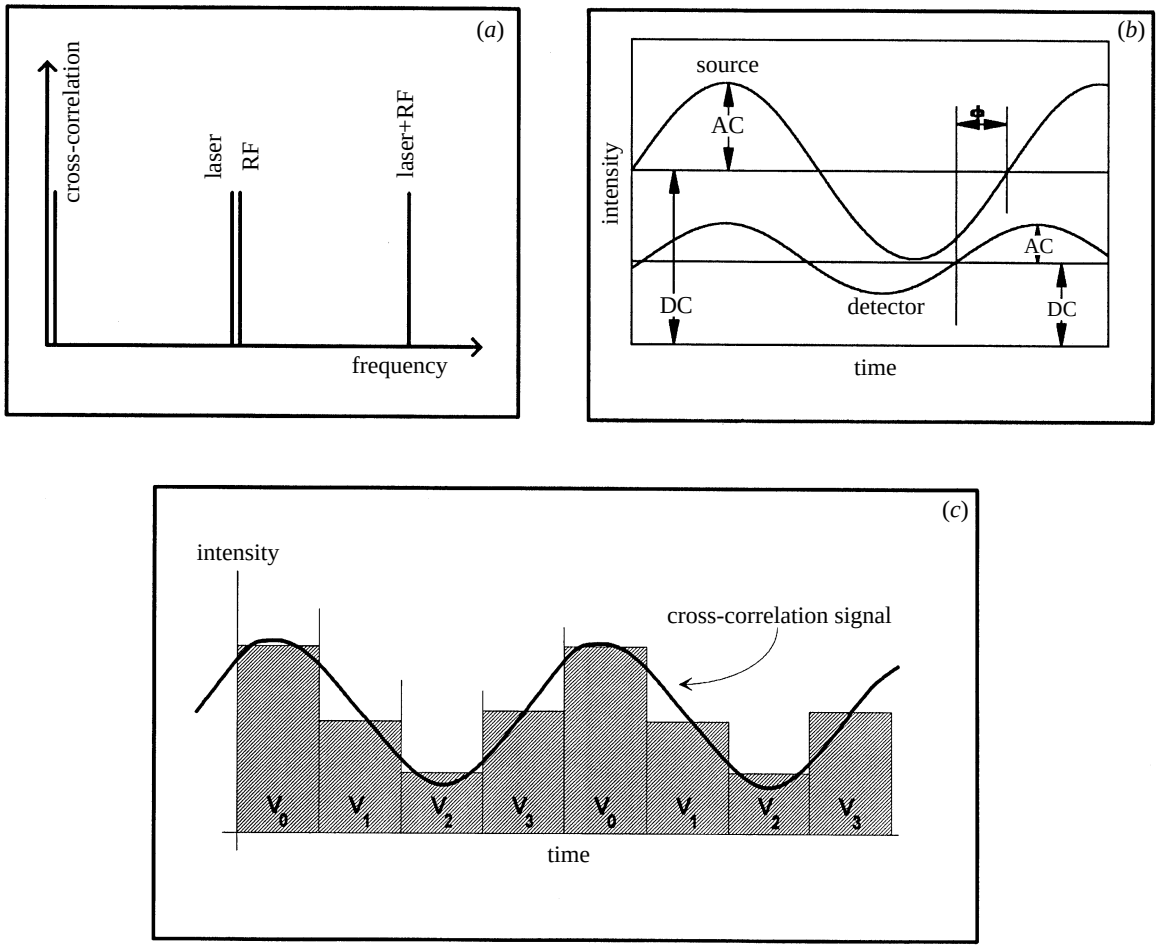

Figure 1. Schematic representation of the frequency-domain acquisition principles. (*a*) A radio-frequency signal (RF) at 120 001 000 Hz is used to modulated the gain of the detector causing down-conversion of the laser frequency at 120 000 000 Hz. The difference frequency between the laser and the radio frequency, 1 kHz, is the cross-correlation frequency. (*b*) The DC, AC and phase of the cross-correlation signal contain the same information as the original high-frequency signal. The signal at the detector is attenuated and phase-shifted with respect to the signal at the source. (*c*) Measurement of four values per period of the cross-correlation signal is sufficient to provide the DC, AC and phase of the signal.

pair of slopes, we can extract the values of the absorption and scattering coefficients according to the following expressions (Fantini *et al.* 1994*a*).

$$\text{Using the DC, phase: } \mu_a = -\frac{\omega}{2v}\frac{S_{DC}}{S_\Phi}\left(\frac{S_\Phi^2}{S_{DC}^2}+1\right)^{-\frac{1}{2}}, \quad (7)$$

$$\mu_s' = \frac{S_{DC}^2}{3\mu_a}. \quad (8)$$

$$\text{Using the AC, phase: } \mu_a = \frac{\omega}{2v}\left(\frac{S_\Phi}{S_{AC}}-\frac{S_{AC}}{S_\Phi}\right), \quad (9)$$

$$\mu_s' = \frac{S_{AC}^2-S_\Phi^2}{3\mu_a}. \quad (10)$$

$$\text{Using DC, AC: } \mu_a = \frac{\omega}{2v}\frac{S_{DC}}{S_{AC}}\left(\frac{S_{AC}^2}{S_{DC}^2}-1\right)^{-\frac{1}{2}}, \quad (11)$$

$$\mu_s' = \frac{S_{DC}^2}{3\mu_a}. \quad (12)$$

There are additional practical advantages of the multidistance method. One of the most important is the relative independence of the slope measurement on the curvature of the surface on which the measurement is made (Cerussi *et al.* 1996). For practical purposes, we have implemented the measurement of the slope of the phase and amplitude by measuring the amplitude and the phase of the photon density wave at four selected distances from the source. A computer algorithm calculates the average scattering and absorption from those slopes. The recovery of μ_a and μ_s' is very accurate and given the nature of the measurement, i.e. measuring a slope rather than a value, μ_a and μ_s' are largely independent from the absorbance of the skin or other local factors (Fantini *et al.* 1994*a*)

Although the equations we have reported are valid in the infinite medium, similar equations can be written for the semi-infinite medium, which better approximate actual measurement techniques (Fantini *et al.* 1994*b*). Generally, measurement of the scattering and absorption coefficients of a particular area of the body can be done non-invasively by placing a light source (emitting light in the near-infrared range—between 700 nm and 1300 nm) and a detector on two points on the surface of the skin, at a distance of a few centimetres apart. Most tissues in the human body are

highly scattering in the near-infrared. For instance, the reduced scattering coefficients of grey and white matters of the adult brain range between 20 and 30 cm^{-1} (for the grey matter) and between 70 and 120 cm^{-1} (for the white matter) (Van der Zee *et al.* 1993). On the contrary, the absorption coefficients of the adult brain are of the order of 0.25 cm^{-1} for the grey matter, and 0.05 cm^{-1} for the white matter (Van der Zee *et al.* 1993). These basic optical properties of head tissues indicate that the Boltzmann transport equation for photons inside the head can be solved in the diffusion approximation (Case & Zweifel 1967; Jacques 1989; Fishkin *et al.* 1991; Madsen *et al.* 1991; Gratton *et al.* 1993; Svaasand *et al.* 1993) and that the propagation of photons through the tissue can be described as a diffusion process (Ishimaru 1978). This has several consequences of practical importance.

The individual photon trajectories form the source to the detector are highly variable and they comprise an extended volume. Modifications in the optical properties occurring within this volume influence the light intensity and the time-of-flight. The size of the volume determines the spatial resolution of the technique (of the order of 1 cm). Due to the diffusive nature of light propagation in tissues, only photons travelling deeply into the medium are likely to reach the detector. The volume explored by a source–detector pair located on the surface of the medium (head) is a curved spindle with an average depth about one-quarter the distance between the source and the detector (Bonner *et al.* 1988; Gratton *et al.* 1994). Therefore, it is possible to study the properties of relatively deep structures (such as the cortex) by placing a source and a detector on the surface of the head. The number of photons reaching the detector (i.e. the attenuation) decreases more than exponentially with the source–detector distance (equation (3)), whereas the phase delay of the photon density wave is linear with distance (equation (2)). In the case of head tissues, the large attenuation of the light limits the maximum useful source–detector distance to less than 10 cm, and effectively limits the maximum penetration depth to less than 5 cm from the surface. For adult heads, also the high absorption of the grey matter can further limit the effective penetration.

The crucial point in the determination of the optical parameters of tissues using the multidistance method is in how well the actual anatomy realize the conditions of a semi-infinite medium. We have demonstrated that the effect of the skin absorption is negligible in the multidistance method, but the effect of large underlying structures such as bones or fat layers, may strongly modify the modalities of light propagation. In particular the relatively clear cerebral fluid layer can strongly affect the modalities of light propagation (Firbank *et al.* 1996). We have performed Monte-Carlo simulations on layered structures to assess how much the multidistance method is affected by the different layers (Gratton *et al.* 1995*b*). The results are quite complex and cannot be easily generalized, since they strongly depend on the optical properties and thickness of the different layers. However, for reasonable parameters of the intervening layers, the multidistance method may provide one of the most robust approaches. For example, figure 2 shows Monte-Carlo simulations of the recovery of the optical parameters of an underlying layer using the multidistance method as a function of the layer depth. In the simulations, the medium has an absorption of 0.043 cm^{-1} and the scattering coefficient has a value of 3.2 cm^{-1}. In the frequency-domain simulation a frequency of 110 MHz for light modulation was used and four detectors spaced by 1 cm with the first one at 3 cm from the light source were used as shown in figure 2*a*. The layer has the same scattering coefficient as the surrounding medium and an absorption of a factor of two larger than the medium ($\mu_a = 0.086\ cm^{-1}$). The layer was then moved in one centimetre steps from the surface (a depth of zero corresponds to no layer) to a depth of 7 cm. The recovered optical parameters are shown in figure 2*b*. For this simple situation, the multidistance method recovers the optical parameters of the layer within 25 % of its value when the layer is at a depth of 2 cm. Of course, for other layer positions, the optical parameters of the layer are not well recovered,

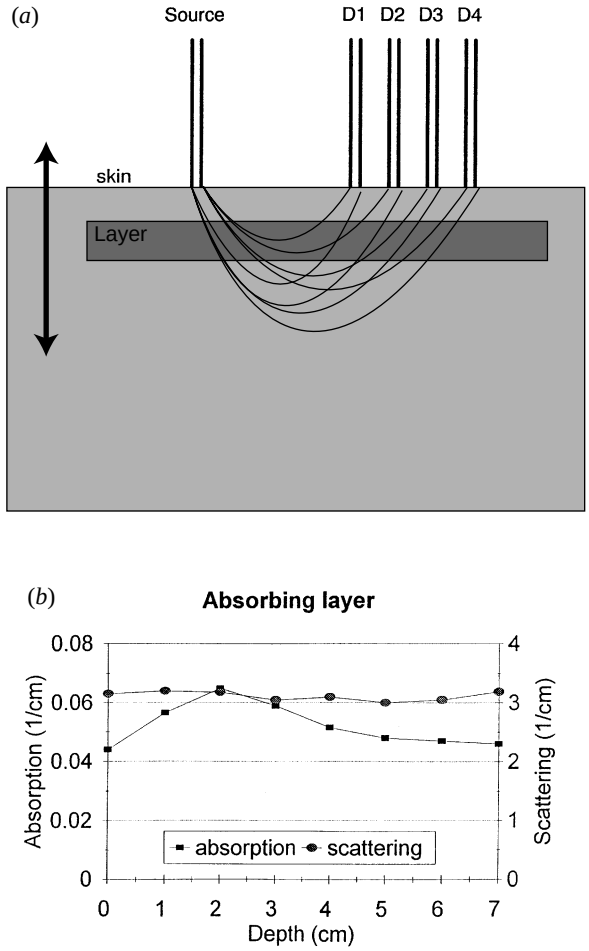

Figure 2. (*a*) Schematics of the multidistance protocol measurement. Four detectors separated by 1 cm and at a minimum distance of 3 cm from the light source are placed on the surface of the scattering medium. In the Monte-Carlo simulation an infinitely long layer is moved in steps of 1 cm from above the surface to a maximum depth of 7 cm. (*b*) Recovered absorption and scattering coefficients using the multidistance protocol for different positions of the layer.

Table 1. *Absorption and reduced scattering coefficients of the human forehead and forearm measured with the frequency-domain multidistance method at 715 and 825 nm*

(From the absorption coefficient data, the haemoglobin saturation (Y) and concentration ($[Hb]_{tot}$) can be derived under the assumption that haemoglobin is the dominant absorber of NIR light.)

	$\lambda = 715$ nm		$\lambda = 825$ nm			
	μ_a (cm^{-1})	μ_s' (cm^{-1})	μ_a (cm^{-1})	μ_s' (cm^{-1})	Y (%)	$[Hb]_{tot}$ (μM)
forehead	0.16	7.3	0.16	6.9	60	80
forearm	0.18	3.7	0.24	3.0	79	120

probably due to the partial intersection of the light bundle with the absorbing layer. Other simulations (not shown) point out that for a layer that is more scattering than the surrounding but that has the same absorption, the recovery of the optical parameters of the layer is not as accurate. As a general comment, only the full solution of the inverse problem will provide the correct medium parameters for a non-homogeneous medium. In the absence of a fast and reliable solution of the inverse problem, and for measurements of small variations in the optical parameters of one of the layers, the multidistance method is one of the less affected by systematic errors due to layer structures. In the case of the measurement of optical parameters of muscle, it appears that the assumptions of a relatively homogeneous mass is well satisfied.

As an example of the operation of our measurement protocol, table 1 reports values of the reduced scattering and absorption coefficients measured with our instrument on the human forearm and forehead (Ferrari *et al*. 1995). By measuring the absorption coefficient at two wavelengths, the haemoglobin saturation (Y) and concentration ($[Hb]_{tot}$) can be determined. These derived values are also reported in table 1. It has recently been proposed that the reduced scattering coefficient of tissues can carry physiologically important information, being possibly related to blood glucose concentration (Kohl *et al*. 1994; Maier *et al*. 1994).

5. MEASUREMENT OF NEURONAL ACTIVITY

Recent studies on exposed cortex have shown that the optical properties of the cortex change when the cortex is functionally active due to absorption and scattering changes (Grinvald *et al*. 1986; Frostig *et al*. 1990; Federico *et al*. 1994; Holthoff *et al*. 1994). Absorption changes are identified with metabolic and haemodynamic phenomena and they are relatively slow (seconds). Scattering changes are less well understood. Studies on isolated neurons (Cohen 1972) and on the nervous systems of invertebrates (Stepnowski *et al*. 1991) have shown that the scattering from neurons change during action potentials (milliseconds). Since near-infrared light can penetrate deeply into tissue, optical methods employing near-infrared radiation could also be used to image internal body structures non-invasively (Chance 1989; Benaron & Stevenson 1993).

In the experiments described, the light source was a light-emitting diode (LED) with a wavelength of 715 nm, and a power of less than 1 mW. The source–detector distance was fixed at 3 cm (computer simulations indicated that this distance allows for the detection of phenomena occurring at a depth of up to 3 cm (Gratton *et al*. 1995*a*)). The phase and the attenuation of the photon density wave were acquired using sampling rates varying between 12.5 and 50 Hz in different experiments. The measurements were obtained using a single-channel system (maps were obtained by repeating measurements at multiple locations).

The pulsation of the vascular system, and in particular of large and medium arteries, that is associated with systolic activity of the heart produces relatively large changes in the transmission of light through tissue (Jennings & Choi 1983). The signal due to pulsation may be quite significant and it is exploited for studying haemodynamic effects related to brain activity. However, when the interest is in detecting neuronal activity, pulsation may produce substantial artefacts that are difficult to eliminate with simple filtering approaches. It is therefore important to separate the changes in intensity due to haemodynamics from the changes due to neuronal activity. We have developed an algorithm for the estimation of the pulse artifact (Gratton & Corballis 1995) based on a regression procedure in which the effect of systolic pulsation is estimated from the data. The basic idea is that pulsation produces a signal that is always self-similar, although it may vary in intensity and duration. Our tests showed that, when used to estimate and subtract the effects of pulsation from the optical recordings, the procedure substantially reduces the impact of the pulsation artefact. This procedure was applied to all our data.

(*a*) *Absorbing and scattering objects can be detected through the skull*

We demonstrated using phantoms that detection of deep structures (4–5 cm) inside a highly scattering medium was possible using non-invasive techniques (Benaron & Stevenson 1993; Gratton *et al*. 1994). A semi-infinite scattering medium bounded by a non-scattering medium was simulated using a tank filled with skimmed milk. Using this phantom, we studied the volume explored by a photon density wave introduced by a source at the surface and detected at another point on the same side of the surface. The

average path followed by photons diffusing from the source to the detector was determined by observing the effects of a small absorbing sphere immersed in the liquid phantom. The placement of the absorbing sphere was varied systematically, and the phase and the amplitude of the photon density wave were measured at each sphere position. The reasoning used in this study was that the absorbing sphere interferes with the measurements only if it intersects the average path followed by the photons. The results confirmed the prediction that photons travelling from the source to the detector follow trajectories which are contained in a banana-shaped region. In addition, the data demonstrated that the volume explored in time-resolved measures was much narrower than that explored in steady-state measures. Some of the results of these initial studies were reported by Gratton *et al.* (1994). Using the same experimental set-up, we showed that by moving the detector at the surface of the scattering medium, a shadow of the absorbing sphere can be easily distinguished by recording the phase and the amplitude of the photon density wave. We further showed that the images of absorbing objects could be obtained through bony structures by placing a small absorbing sphere inside a sheep's skull (Gratton *et al.* 1994). The skull was then submerged in skimmed milk. The surface of the milk was scanned using a source–detector pair. The image obtained with the sphere inside the skull was compared with an image obtained without the sphere. The difference between the two images indicated that structures with specific optical properties can be visualized through the skull. In addition we proved that scattering objects give larger signals than absorbing objects.

(*b*) *Non-invasive measurement of brain activity: distinction between fast and slow effects*

Several studies have shown that functional changes of brain activity can be detected by optical methods based on measures of propagation of photon density waves (Chance *et al.* 1993; Hoshi & Tamura 1993; Obrig *et al.* 1994; Gratton *et al.* 1995*a*, *b*; Maki *et al.* 1995; Meek *et al.* 1995). Two types of changes have been reported: *fast effects* (with a 50–500 ms latency) and *slow effects* (with a 2–10 s latency). These two effects have probably different origins and they can be distinguished because of their large difference in time-scale. Also slow and fast effects are measured in a different ways. Slow changes of the optical parameters are observed by using a sustained activation task, such as one involving repeated stimulation (or repeated movements). A similar approach is used for functional magnetic resonance imaging (fMRI) and positron emission tomography (PET) (Belliveau *et al.* 1991). Fast changes of optical parameters are detected by averaging the time course of the activity elicited by (or associated with) individual stimulation. This approach is used for ERPs and MEG. More importantly, fast and slow effects differ in terms of the optical parameters they affect. Slow effects can be observed using both steady-state and time-resolved methods (see Hoshi & Tamura 1993; Obrig *et al.* 1994; Gratton *et al.* 1995*a*; Maki *et al.* 1995). Instead, fast effects are best visualized using time-resolved methods (see Gratton *et al.* 1995*a*, *b*; Meek *et al.* 1995).

To a large extent, the slow effects can be attributed to the changes of absorption that are probably produced by oxygenation and haemodynamic changes which occur in active areas of the brain (Obrig *et al.* 1994; Villringer & Dirnagl 1995). They may also be related to the effects observed with PET studies of blood flow, although the time-course of the latter cannot be studied with the same level of detail.

(*c*) *Detection of fast optical signals*

We have used several protocols to stimulate fast optical signal (Gratton *et al.* 1995*a*, *b*; Gratton *et al.* 1996; Fabiani *et al.* 1996). Our studies indicate that fast signals may reflect localized neuronal activation related to specific stimulation (or preparation for movement). Using the location where fast signals are observed, we have obtained maps demonstrating spatial resolution of at least 5 mm. In other studies using visual stimulation we showed that changes in the brain optical parameters can distinguish between stimulation effects (localized to area 17) and attention effects (that are evident in extrastriate areas of the occipital cortex). Furthermore we demonstrated that the localization of fast optical signal shows spatial correspondence with fMRI data and temporal correspondence with visual evoked potential data collected in the same paradigm.

We (Gratton *et al.* 1995*a*) recorded fast optical signals (with detectors placed on the surface of the head directly above the two motor cortices, and the light source placed on the vertex), while subjects were performing a task in which they were required to tap one hand or one foot at regular intervals. Because of the neuroanatomical characteristics of the primary motor cortex (in which the right motor strip controls movements in the left part of the body and vice versa), differential effects were expected for hand movements that were contralateral or ipsilateral to the location of the detector. Specifically, it was hypothesized that when the detector was placed on the side contralateral to the hand movement, the photon path should cross motor areas in which neurons were active. In this study, four subjects were asked to tap one of their hands for 10 s at a frequency of 0.8 Hz; 10 s of rest preceded and followed the tapping period. As expected, systematic differences in the photon delay parameter emerged as a function of side movement, consisting of changes occurring at the tapping frequency (0.8 Hz) and/or its harmonics.

The tapping experiment had several limitations. Specifically, maps of activity could not be derived from the data because only two locations (one above each of the motor strips) were tested. In addition, the data recording was not time-locked with the tapping movements of the subjects. In further studies we address these problems (Gratton *et al.* 1995*b*) to determine whether fast optical signals could be used to derive a retinotopic map of the primary visual cortex. To gain more understanding of the time course of the

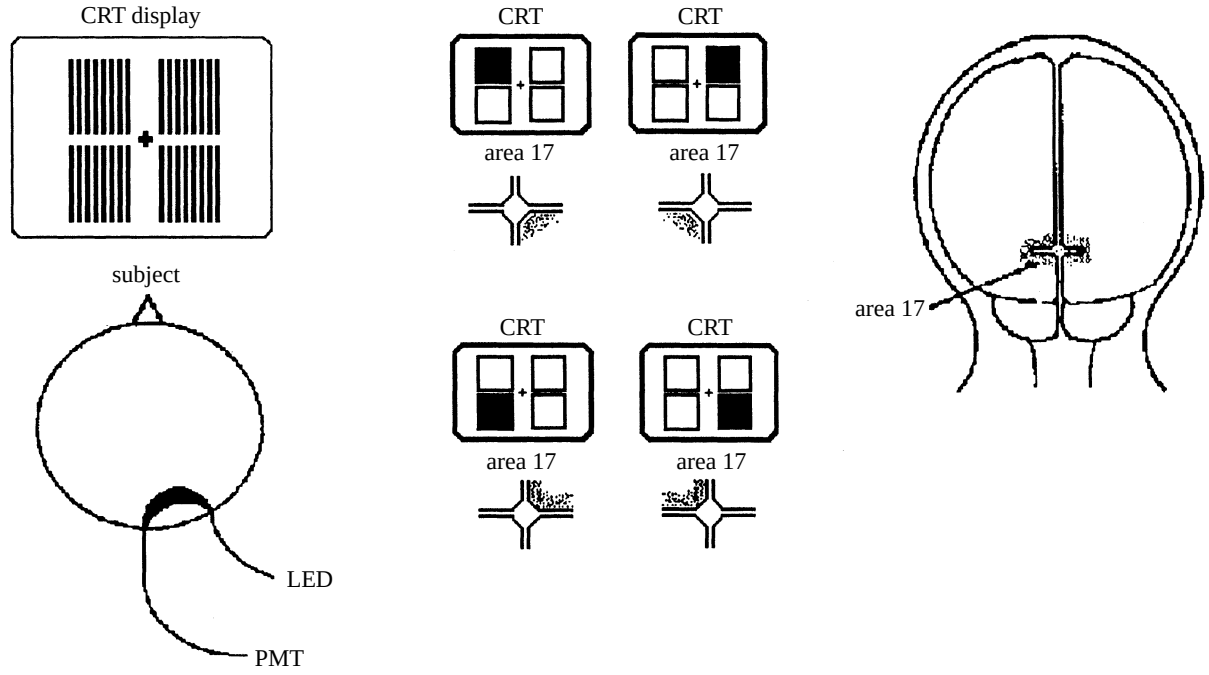

Figure 3. Schematic representation of the measurement protocol for the visual stimulus experiments. A light source (LED) and a detector optical fibre are placed on the head in contact with the skin in different positions corresponding to different areas of the visual cortex. The subject observes a changing pattern on the screen. Data acquisition is synchronized with the pattern change. Four different patterns are used to stimulate different areas of the visual cortex.

fast optical signal, a faster sampling rate (20 Hz) was employed and the recording of the optical parameters was time-locked to the presentation of visual stimuli. The stimuli consisted of four black-and-white vertical grids, displayed in the four quadrants of a computer monitor. On each trial, one of the grids switched colours every 500 ms, while the alternating grid was varied across trials. This was expected to produce systematic variations in the segment of primary visual cortex being stimulated on each trial. Photon migration parameters (light intensity and delay) were measured from 12 scalp locations over the occipital lobe, to obtain a map of the visual cortex. Average waveforms corresponding to the changes in optical parameters during the first 500 ms after stimulation were derived. The analyses identified a deflection in the delay parameter, peaking 100 ms after stimulation and reaching a maximum delay of about 10 ps. The maps obtained with these data (reported by Gratton *et al.* (1995*b*)) indicate that the areas of maximum response for each of the four stimulation conditions correspond to the expected retinotopic map of the visual field in primary visual cortex (i.e. the maps are inverted along both the vertical and horizontal axes). Direct data on the depth of these effects are not available. However, simulations reported by Gratton *et al.* (1995*a*) suggest that changes of about 10 ps in the delay parameter, combined with virtually no change in the intensity parameter, are consistent with variations in scattering (or absorption) of layers located at a depth of 1.5–3 cm (which corresponds to the depth of the superficial half of the primary visual cortex). The latency of the effects appear consistent with the idea that they may be due to the scattering changes ensuing in conjunction with electrical neuronal activity, as proposed by Stepnoski *et al.* (1991; see also Frostig 1994). The time resolution of the optical measurement can be as high as 1 ms, using our current instrument (figures 3 and 4).

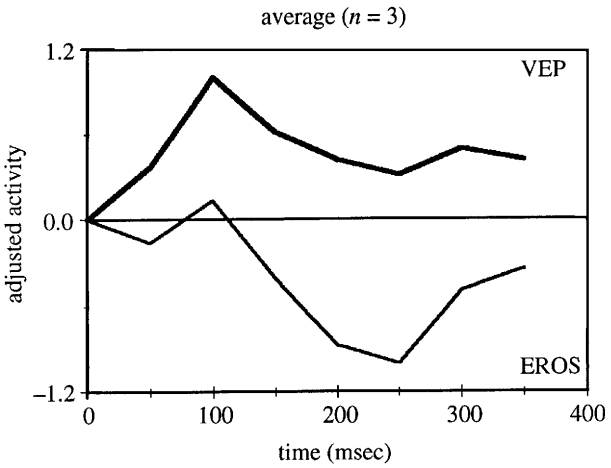

Figure 4. Temporal superposition of the electric evoked potentials (VEPs) and of the optical signal changes (EROS) in the region of maximum stimulus for three different subjects and the average of all the subjects. The electrical and optical signals have a similar time-course.

6. CONCLUSIONS

The results from our studies of fast changes of optical properties suggest that this signal occurs simultaneously with or before the surface electrical potential (evoked potential or ERP). This makes the fast optical signal an ideal marker for indexing the occurrence of neuronal activity. The fast optical signal also appears to be very localized, so as to allow

different parts of the same neuroanatomical area of the cortex (as in the case of Brodmann's area 17) to be distinguished. Our data indicate that this localization is consistent with that obtained using fMRI. This may be useful in two ways. (i) It may help us when studying the relative timing of neuronal activity in different brain areas. This may have profound theoretical implications, since we expect most brain functions (such as vision, memory, attention, language, movement control, etc.) to depend on the dynamic interactions between different brain areas. (ii) The possibility of deriving data with high resolution both in the temporal and the spatial domains may help the integration of various non-invasive methods for studying brain function, and in particular electrophysiological and haemodynamic techniques.

Although non-invasive optical methods are quite promising for the study of brain function, it is also clear that these methods have intrinsically limited spatial resolution. However, the temporal resolution can be further improved to parallel the temporal resolution of electrical signals. So far our data are constrained by methodological issues, some of which appear solvable, others beyond the capabilities of non-invasive measurements using photon density waves. The lack of tridimensional reconstruction can, in principle, be solved using a reconstruction algorithm. Another important consideration is the lack of understanding of the origin of the signal observed. At present we have not proved what causes the changes of the phase delay upon activation of certain parts of the brain.

This work is supported by NIH grants RR03155 and CA57032, and also a joint Whitaker–NIH grant RR10966.

REFERENCES

Benaron, D. A. & Stevenson, D. K. 1993 Optical time-of-flight and absorbance imaging of biologic media. *Science* **259**, 1463–1466.

Belliveau, J. W., Kennedy, D. N., Mckinstry, R. C. & Buchbinder, B. R. 1991 Functional mapping of the human visual cortex by magnetic resonance imaging. *Science* **254**, 716–719.

Bonner, R. F., Nossal, R. & Havlin, S. 1988 Model for photon migration in turbid biological media. *J. Opt. Soc. Am.* A **4**, 423–432

Case, K. M. & Zweifel, P. F. 1967 *Linear transport theory*. Reading, MA: Addison-Wesley.

Cerussi, A., Maier, J., Fantini, S., Franceschini, M. A. & Gratton, E. 1996 The frequency-domain multi-distance method in the presence of curved boundaries. In *OSA trends in optics and photonics on biomedical optical spectroscopy and diagnostics*, vol. 3 (ed. E. Sevick-Muraca & D. Benaron), pp. 92–97. Washington, DC: Optical Society of America.

Chance, B. 1989 *Adv. Exp. Med. Biol.* **248**, 21–31.

Chance, B. 1991 Optical method. *A. Rev. Biophys. Biophys. Chem.* **20**, 1–28.

Chance, B., Zhuang, Z., UnAh, C., Alter, C. & Lipton, L. 1993 Cognition-activated low-frequency modulation of light absorption in human brain. *Proc. Natn. Acad. Sci. USA* **90**, 3423–3427.

Cohen, L. B. 1972 Changes in neuron structure during action potential propagation and synaptic transmission. *Physiol. Rev.* **53**, 373–417.

Fabiani, M., Gratton, G., Hirsch, J., Corballis, P. M., Goodman, M., Friedman, D. & Hood, D. 1996 Converging on the brain: a combined optical, fMRI, and evoked potential study of activity in the human primary visual cortex.

Fantini, S., Franceschini, M. A., Fishkin, J. B., Barbieri, B. & Gratton, E. 1994*a* Quantitative determination of the absorption spectra of chromophores in strongly scattering media: a light-emitting-diode based technique. *Appl. Opt.* **33**, 5204–5213.

Fantini, S., Franceschini, M. A. & Gratton, E. 1994*b* Semi-infinite-geometry boundary problem for light migration in highly scattering media: a frequency-domain study in the diffusion approximation. *J. Opt. Soc. Am.* B **11**, 2128–2138.

Fantini, S., Franceschini, M. A. & Gratton, E. 1997 Effective source term in the diffusion equation for photon transport in turbid media. *Appl. Opt.* **36**, 156–163.

Fantini, S., Franceschini, M. A., Maier, J. S., Walker, S. A., Barbieri, B. & Gratton, E. 1995 Frequency-domain multichannel optical detector for non-invasive tissue spectroscopy and oximetry. *Opt. Eng.* **34**, 32–42.

Federico, P., Borg, S. G., Salkauskus, A. G. & MacVicar, B. A. 1994 Mapping patterns of neuronal activity and seizure propagation by imaging intrinsic optical signals in the isolated whole brain of the guinea-pig. *Neuroscience* **58**, 461–480.

Ferrari, M., De Blasi, R. A., Fantini, S., Franceschini, M. A., Barbieri, B., Quaresima, V. & Gratton, E. 1995 Cerebral and muscle oxygen saturation measurement by a frequency-domain near-infrared spectroscopic technique. *Proc. SPIE* **2389**, 868–874.

Firbank, M., Arridge, S. R., Schweiger, M. & Delpy, D. T. 1996 An investigation of light transport through scattering bodies with non scattering regions. *Phys. Med. Biol.* **41**, 767–783.

Fishkin, J. B. and Gratton, E. 1993 Propagation of photon-density waves in strongly scattering media containing an absorbing semi-infinite plane bounded by a straight edge. *J. Opt. Soc. Am.* A **10**, 127–140.

Fishkin, J., Gratton, E., van de Ven, M. J. & Mantulin, W. W. 1991 Diffusion of intensity modulated near-IR light in turbid media. In *Time-resolved spectroscopy and imaging of tissues* (ed. B. Chance), *Proc. SPIE* **1431**, 122–123.

French, T. 1996 Thesis, University of Illinois at Urbana-Champaign.

Frostig, R. D. 1994 What does *in vivo* optical imaging tell us about the primary visual cortex in primates? In *Cerebral Cortex* (ed. A. Peters & K. S. Rockland), pp. 331–358. New York: Plenum Press.

Frostig, R. D., Lieke, E. E., Ts'o, D. Y. & Grinvald, A. 1990 Cortical functional architecture and local coupling between neuronal activity and the microcirculation revealed by *in vivo* high-resolution optical imaging of intrinsic signals. *Proc. Natn. Acad. Sci., USA* **87**, 6082–6086.

Gratton, G. & Corballis, P. M. 1995 Removing the heart from the brain: compensation for the pulse artifact in photon migration signals. *Psychophysiology* **32**, 292–299.

Gratton, G., Corballis, P. M., Cho, E., Fabiani, M. & Hood, D. C. 1995*a* Shades of gray matter: noninvasive optical images of human brain responses during visual stimulation. *Psychophysiology* **32**, 505–509.

Gratton, G. Fabiani, M. & Corballis, P. M. 1996 Can we measure correlates of neuronal activity with non-invasive optical methods? In *Optical imaging of brain function and metabolism: physiological basis and comparison to other functional neuroimaging methods. Advances in experimental medicine and biology* (ed. A. Villringer & U. Dirnagl). New York: Plenum Press.

Gratton, G., Fabiani, M., Friedman, D., Franceschini, M. A., Fantini, S., Corballis, P. M. & Gratton, E. 1995*b* Rapid

changes of optical parameters in the human brain during a tapping task. *J. Cogn. Neurosci.* **7**, 1446–1456.

Gratton, E. & Limkeman, M 1983 A continuously variable frequency cross-correlation phase fluorometer with picoseconds resolution. *Biophys. J.* **44**, 315–324.

Gratton, E., Jameson, D. N., Rosato, N. & Weber, G. 1984 Multifrequency cross-correlation phase fluorometer using synchrotron radiation. *Rev. Scient. Instrum.* **55**, 486–493.

Gratton, G., Maier, J. S., Fabiani, M., Mantulin, W. W. & Gratton, E. 1994 Feasibility of intracranial near-infrared optical scanning. *Psychophysiology* **31**, 211–215.

Gratton, E., Mantulin, W. W., van de Ven, M. J., Fishkin, J. B., Maris, M. B. & Chance, B. 1993 A novel approach to laser tomography. *Bioimaging* **1**, 40–46.

Grinvald, A., Lieke, E., Frostig, R. D., Gilbert, C. D. & Wiesel, T. N. 1986 Functional architecture of cortex revealed by optical imaging of intrinsic signals. *Nature* **324**, 361–364.

Holthoff, K., Dodt, H. U. & Witte, O. W. 1994 Changes in intrinsic optical signal of rat neocortical slices following afferent stimulation. *Neurosci. Lett.* **180**, 227–230.

Hoshi, Y. & Tamura, M. 1993 Dynamic multichannel near-infrared optical imaging of human brain activity. *J. Appl. Physiol.* **75**, 1842–1846.

Ishimaru, A. 1978 *Wave propagation and scattering in random media*, vol. 1. New York: Academic Press.

Jacques, S. L. 1989 Time-resolved propagation of ultra short laser pulses within turbid tissues. *Appl. Opt.* **28**, 2223–2229.

Jennings, J. R. & Choi, S. 1983 An arterial to peripheral pulse wave velocity measure. *Psychophysiology* **20**, 410–418.

Kohl, M., Cope, M., Essenpreis, M. & Böcker, D. 1994 Influence of glucose concentration on light scattering in tissue-simulating phantoms. *Opt. Lett.* **19**, 2170–2172.

Maier, J. S., Walker, S. A., Fantini, S., Franceschini, M. A. & Gratton, E. 1994 Possible correlation between blood glucose concentration and the reduced scattering coefficient of tissues in the near infrared. *Opt. Lett.* **19**, 2062–2064.

Madsen, S. J., Patterson, M. S., Wilson, B. C., Park, Y. D., Moulton, J. D., Jacques, S. L., Anderson, M. D. & Hefetz, Y. 1991 Time-resolved diffuse reflectance and transmittance studies in tissue simulating phantoms: a comparison between theory and experiments. In *Time-resolved spectroscopy and imaging of tissues* (ed. B. Chance), *Proc. SPIE* **1431**, 42–51.

Maki, A., Yamashita, Y., Ito, Y., Watanabe, E., Mayanagi, Y. & Koizumi, H. 1995 Spatial and temporal analysis of human motor activity using noninvasive NIR topography. *Med. Phys.* **22**, 1997–2005.

Meek, J. H., Elwell, C. E., Khan, M. J., Romaya, J., Wyatt, J. S., Delpy, D. T. & Zeki, S. 1995 Regional changes in cerebral haemodynamics as a result of visual stimulus by near infrared spectroscopy. *Proc. R. Soc. Biol. Sci.* **261**, 351–356.

Obrig, H., Wolf, T., Dirnagl, U. & Villringer, A. 1994 The cerebral hemoglobin oxygenation response depends on stimulus modality and is modulated by blood glucose concentration. 22nd Annual Meeting of ISOTT, August 1994, Istanbul, Turkey.

O'Leary, M. A., Boas, D. A., Chance, B. & Yodh, A. G. 1992 Refraction of diffuse photon density waves. *Phys. Rev. Lett.* **69**, 2658–2661.

Patterson, M. S., Chance, B. & Wilson, B. C. 1989 Time-resolved reflectance and transmittance for the non-invasive measurement of tissue optical properties. *Appl. Opt.* **28**, 231–236.

Pogue, B. W. 1995 Frequency-domain optical spectroscopy and imaging of tissue and tissue-simulating media. Ph.D. Thesis, McMaster University, Hamilton, Ontario, Canada.

Stepnowski, R. A., LaPorta, A., Raccuia-Behling, F., Blonder, G. E., Slusher, R. E. & Kleinfeld, D. 1991 Non-invasive detection of changes in membrane potential in cultured neurons by light scattering. *Proc. Natn. Acad. Sci. USA* **88**, 9382–9386.

Svaasand, L. O., Haskell, D., Tromberg, B. & McAdams, M. 1993 Properties of photon density waves at boundaries. *Proc. SPIE* **1888**, 214–226.

Van der Zee, P., Essenpreis, M. & Delpy, D. T. 1993 Optical properties of brain tissue. *Proc. SPIE* **1888**, 454–465.

Villringer, A. & Dirnagl, U. 1995 Coupling of brain activity and cerebral blood flow: basis of functional neuroimaging. *Cerebrovasc. Brain Metab. Rev.* **7**, 240–276.

Wilson, B. C, Patterson, M. S. & Flock, S. T. 1987 Indirect versus direct techniques for the measurement of optical properties of tissues. *Photochem. Photobiol.* **46**, 601–608.